

1 **Immobilization of Baeyer-Villiger monooxygenase from acetone grown *Fusarium* sp.**

2  
3 Michio Takagi<sup>1</sup>, Kotchakorn T.sriwong<sup>1</sup>, Ayaka Masuda<sup>1</sup>, Nozomi Kawaguchi<sup>1</sup>, Shusuke Fukui<sup>1</sup>, Huong  
4 Le Viet Lan<sup>1</sup>, Dai-ichiro Kato<sup>2</sup>, Takashi Kitayama<sup>3</sup>, Mikio Fujii<sup>4</sup>, Afifa Ayu Koesoema<sup>5</sup>, Tomoko  
5 Matsuda<sup>1\*</sup>

6  
7 <sup>1</sup>Department of Life Sciences and Technology, School of Life Science and Technology, Tokyo Institute of  
8 Technology, 4259 Nagatsuta-cho, Midori-ku, Yokohama, 226-8501, Japan

9  
10 <sup>2</sup>Graduate School of Science and Engineering, Kagoshima University  
11 1-21-35 Korimoto, Kagoshima 890-0065 Japan  
12 k0035454@kadai.jp

13  
14 <sup>3</sup>Faculty of Agriculture, Kindai University  
15 3327-204, Nakamachi, Nara, Japan  
16 kitayama@nara.kindai.ac.jp

17  
18 <sup>4</sup>School of Pharmacy, International University of Health and Welfare  
19 2600-1 Kitakanemaru, Ohtawara, Tochigi, Japan  
20 mfujii@iuhw.ac.jp

21  
22 <sup>5</sup>Research Institute for Interdisciplinary Science (RIIS), Okayama University  
23 700-8530 3-1-1 Tsushimanaka, Kita-ku, Okayama-shi, Japan

24  
25 Corresponding author:

26 Tomoko Matsuda (tmatsuda@bio.titech.ac.jp, tel/fax +81-45-924-5757)

27  
28  
29 **Abstract**

30 *Objective*

31 A novel biocatalyst for Baeyer–Villiger oxidations is necessary for pharmaceutical and chemical  
32 industries, so this study aims to find a Baeyer–Villiger monooxygenase (BVMO) and to improve its  
33 stability by immobilization.

34 *Results*

35 Acetone, the simplest ketone, was selected as the only carbon source for the screening of microorganisms  
36 with a BVMO. A eukaryote, *Fusarium* sp. NBRC 109816, with a BVMO (*FBVMO*), was isolated from a  
37 soil sample. *FBVMO* was overexpressed in *E. coli* and successfully immobilized by the organic-inorganic  
38 nanocrystal formation method. The immobilization improved the thermostability of *FBVMO*. Substrate

39 specificity investigation revealed that both free and immobilized FBVMO were found to show catalytic  
40 activities not only for Baeyer–Villiger oxidation of ketones to esters but also for oxidation of sulfides to  
41 sulfoxides. Furthermore, a preparative scale reaction using immobilized FBVMO was successfully  
42 conducted.

### 43 *Conclusions*

44 FBVMO was discovered from an environmental sample, overexpressed in *E. coli*, and immobilized by  
45 the organic-inorganic nanocrystal formation method. The immobilization successfully improved its  
46 thermostability.

47

### 48 **Keywords**

49 Baeyer-Villiger monooxygenase, *Fusarium* sp. NBRC 109816, immobilization, thermostability

50

51

### 52 **Introduction**

53 The Baeyer–Villiger oxidation (BVO), the transformation of an acyclic ketone or cyclic ketone  
54 to the corresponding ester or lactone, respectively, is an important organic reaction for pharmaceutical  
55 and chemical industries. However, commonly used oxidants for BVO, such as *meta*-chloroperbenzoic  
56 acid (*m*CPBA) and trifluoroperacetic acid (TFPAA) (Know 1993), are potentially explosive. Moreover,  
57 the stoichiometric amounts of hazardous reagent, a peroxyacid, is converted to a carboxylic acid,  
58 producing chemical waste. Therefore, an effort to use environmentally benign oxidants such as H<sub>2</sub>O<sub>2</sub> and  
59 O<sub>2</sub> has been made (Bryliakov 2017; Liu et al. 2020). On the other hand, biocatalysts have been considered  
60 to be sustainable catalysts (Matsuda 2017; Dong et al. 2018; Sheldon and Woodley 2018; Birolli et al.  
61 2019; Wu et al. 2020; Koesoema et al. 2020). For biocatalytic BVO, Baeyer–Villiger monooxygenase  
62 (BVMO) can use oxygen in the air as an oxidant, producing water as a byproduct (Fig. 1), so that the  
63 reactions are not explosive (Morii et al. 1999; Kyte et al. 2004; Rehdorf et al. 2007; Franceschini et al.  
64 2012; Leipold et al. 2012, 2013; Fürst et al. 2017, 2019; Nguyen et al. 2017; Fordwour et al. 2018; Woo  
65 et al. 2018). Approximately a hundred of BVMOs (Fürst et al. 2019) such as *Acinetobacter*  
66 cyclohexanone monooxygenase (*Ac*CHMO)(Donoghue et al. 1976; Chen et al. 1988; Bong et al. 2018),  
67 *Pseudomonas putida* 2,5-diketocamphane monooxygenase (2,5-DKCMO) (Cassimjee et al. 2014), and  
68 *Thermocrispum municipale* cyclohexanone monooxygenase (*Tm*CHMO) (Delgove et al. 2019) have been  
69 used for biocatalytic BVO. However, comparing other kinds of biocatalysts such as lipases and carbonyl  
70 reductases, the number of available BVMOs are limited, so that there is a high demand to expand on the  
71 diversity (Fürst et al. 2019). Moreover, most of the research with isolated enzymes investigated  
72 prokaryotic BVMOs (Fürst et al. 2019); therefore, eukaryotic BVMOs are lacking (Leipold et al. 2012).

73 While many BVMOs have been discovered by genome mining (Fürst et al. 2019), the potential  
74 of catalytic BVO activity found in the environments by function-driven screening is still underexplored.  
75 Therefore, this study aims to find a unique BVMO from environments. Acetone, the simplest ketone, was  
76 used as the only carbon source, expecting that the simplest substrate is the best to apply for further

77 development. Besides being the simplest, the three acetone metabolic pathways, including BVO,  
78 carboxylation to form acetoacetate, and terminal hydroxylation to form acetol (1-hydroxy-2-propanone),  
79 have been reported (Hausinger 2007). Therefore, acetone was used as the only carbon source for  
80 screening microorganisms with a BVMO in this study, resulting in the isolation of two species of  
81 *Fusarium*, eukaryote, with a BVMO from soil samples. The BVMO from one of them, *Fusarium* sp.  
82 NBRC 109816 (FBVMO), was overexpressed in *E. coli*.

83 Then, FBVMO was immobilized to improve stability since one of the major obstacles for the  
84 utilization of BVMO for organic synthesis is its low stability. So far, BVMOs have not been successfully  
85 immobilized due to their low stability, except in a few cases (Cassimjee et al. 2014; Delgove et al. 2019).  
86 A thermostable cyclohexanone monooxygenase from *Thermocrisum municipale* (TmCHMO) was co-  
87 immobilized on an amino-functionalized agarose-based support with a glucose dehydrogenase (GDH)  
88 (Delgove et al. 2019). 2,5-Diketocamphane monooxygenase from *Pseudomonas putida* (2,5-DKCMO)  
89 was co-immobilized on controlled porosity glass (CPG) with two cofactor-reconverting enzymes  
90 (Cassimjee et al. 2014). Among enzyme immobilization methods (Liese and Hilterhaus 2013; Mohamad  
91 et al. 2015; Basso and Serban 2019; T.sriwong et al. 2021a), the protein-inorganic nanocrystal formation  
92 method is one of the simplest and most effective methods (Ge et al. 2012; Yin et al. 2015; Zhang et al.  
93 2020). Lipase (Zhang et al. 2020), peroxidases (Ge et al. 2012; Yu et al. 2015; Altinkaynak et al. 2016),  
94 alcohol dehydrogenases (López-Gallego and Yate 2015; T.sriwong et al. 2020), and aldehyde  
95 dehydrogenase (T.sriwong et al. 2021b) have been immobilized by this method, achieving the  
96 improvement in the activity and/or stability. However, no BVMO has been immobilized by this method,  
97 to the best of our knowledge. Therefore, immobilization of FBVMO by the method was conducted in this  
98 study, resulting in a significant improvement in thermostability. Substrate specificity investigation  
99 revealed that both free and immobilized FBVMO were found to show catalytic activities not only for  
100 BVO of ketones to esters but also for oxidation of sulfides to sulfoxides. Furthermore, a preparative scale  
101 reaction using immobilized FBVMO was successfully conducted.

102

## 103 **Materials and methods**

### 104 **Reagents, materials, and apparatus**

105 Materials written in the Supplementary Information were used.

106

### 107 **Screening of microorganism using acetone as the only carbon source**

108 Environmental samples from soil, river, and ponds were collected, and diluted by 1.0-10<sup>5</sup> times  
109 with sterilized water, and cultivated at 30 °C and 250 rpm in a liquid medium (Wiegant and De Bont  
110 1980) at pH 7.0 consisting of K<sub>2</sub>HPO<sub>4</sub> (1.55 g/L), KH<sub>2</sub>PO<sub>4</sub> (0.97 g/L), NH<sub>4</sub>Cl (2.0 g/L), MgCl<sub>2</sub>·6H<sub>2</sub>O  
111 (0.075 g/L), (NH<sub>4</sub>)<sub>2</sub>SO<sub>4</sub> (0.10 g/L), NaCl (0.39 g/L), FeSO<sub>4</sub>·7H<sub>2</sub>O (0.010 g/L), ZnSO<sub>4</sub>·7H<sub>2</sub>O (0.010 g/L),  
112 MnSO<sub>4</sub>·5H<sub>2</sub>O (0.010 g/L), KHCO<sub>3</sub> (0.50 g/L), and acetone (50-300 mM). Out of 300 samples, two  
113 microorganisms were able to grow with acetone as the only carbon source. They were identified as  
114 *Fusarium* sp. and *Fusarium oxysporum* Schldtl based on morphological tests (Supplementary Fig. 1) and

115 ITS-5.8S rDNA sequencing. *Fusarium* sp. was deposited to the National Institute of Technology and  
116 Evaluation (Tokyo, Japan) as *Fusarium* sp. NBRC 109816.

117

### 118 **Isolation of the gene**

119 Among the known genomic sequences of various *Fusarium* species, *F. oxysporum* f. sp.  
120 conglutinans race 2 54008 (accession number AGNF01000703.1) was selected by searching a genome  
121 with the highest homology with one of the most studied BVMO, CHMO from *Acinetobacter* sp.  
122 NCIMB9871 (Donoghue et al. 1976). To determine the sequence of FBVMO, four sets of primers  
123 (Supplementary Table 1) were constructed based on the sequence of AGNF01000703.1. for PCR using  
124 the genetic DNA of *Fusarium* sp. NBRC 109816 as a template. To remove the intron, two sets of primers  
125 (Supplementary Table 1) were constructed for PCR using the genetic DNA of *Fusarium* sp. NBRC  
126 109816 as a template. The two PCR products were inserted into pUC19 and transformed into *E. coli*  
127 DH5 $\alpha$ . Another set of primers (Supplementary Table 1) was used for PCR with pUC19-FBVMO as a  
128 template to obtain FBVMO gene to construct pET-21b(+)-FBVMO, which was transformed into *E. coli*  
129 BL21(DE3).

130

### 131 **Overexpression**

132 A single colony of the recombinant cells, BL21(DE3)-pET-21b(+)-FBVMO, was inoculated in  
133 LB medium (4.0 mL) with carbenicillin (125  $\mu$ g/mL) at 250 rpm at 37 °C to an optical density at 600 nm  
134 (OD<sub>600</sub>) reached 0.8-1.0. The pre-cultured cells (2.5 mL) were transferred into LB medium (250 ml) with  
135 carbenicillin (125  $\mu$ g/mL), and cultivated at 250 rpm at 37 °C until OD<sub>600</sub> reached 0.5-0.6. Then, IPTG  
136 (0.2 mM) was added and cultivated at 250 rpm at 18 °C for 18 h. The cells were harvested by  
137 centrifugation at 10,000 G for 5 min at 4 °C, washed with 0.8% NaCl, and suspended in a sodium  
138 phosphate buffer (30 mL, pH 7.4, 20 mM) containing imidazole (5 mM), PMSF (1 mM), and DTT (1  
139 mM). The mixture was sonicated at 100 W for 20 min at 0 °C and centrifuged at 15,000 G for 30 min at 4  
140 °C, and the supernatant (30 mL) was used as a cell-free extract for further study.

141

### 142 **Purification**

143 The cell-free extract (30 mL) was loaded onto a HisTrap<sup>TM</sup>FF crude equilibrated with a sodium  
144 phosphate buffer (pH 7.4, 20 mM) with PMSF (0.2 mM), and DTT (0.2 mM). The bound protein was  
145 eluted by the buffers with 5 mM imidazole (20 mL), 10 mM imidazole (10 mL), 20 mM imidazole (10  
146 mL), 30 mM imidazole (5 mL), and the FBVMO was eluted by the buffer with 70 mM imidazole (5 mL)  
147 with PMSF (0.2 mM), and DTT (0.2 mM). The protein was concentrated by ultrafiltration using Amicon  
148 Ultra-4 10-K MWCO and used for further study. The protein concentration was measured by the Bradford  
149 method (Bradford 1976) using bovine serum albumin (BSA) as a standard. The purification steps are  
150 summarized in Supplementary Table 2.

151

152

153 **Activity measurement of the free enzyme**

154 Cyclohexanone solution (10  $\mu$ L, 0.1 M solution with 10 % diethylene glycol (final  
155 concentration 1 mM)) and sodium phosphate buffer (968  $\mu$ L, pH 7.4, 50 mM) were mixed, and then  
156 NADPH solution (12  $\mu$ L, 10 mg/mL), and purified enzyme (10  $\mu$ L, 1.6-2.0 U/ml) were added. Initial  
157 velocity was determined by following NADPH consumption at 340 nm for 3 min. Activity assays were  
158 done at 25°C in duplicate in a 1.0 mL scale. One unit of enzyme is defined as  $\mu$ mol of NADPH produced  
159 in 1 min under the above conditions.

160

161 **Immobilization**

162 The purified *FBVMO* was immobilized with a similar method to our previous study (T.sriwong  
163 et al. 2020, 2021b). The phosphate-buffer saline (PBS) was prepared by dissolving NaCl (0.80 g), KCl  
164 (0.020 g), Na<sub>2</sub>HPO<sub>4</sub> (0.142 g), and KH<sub>2</sub>PO<sub>4</sub> (0.024 g) in distilled water (100 mL) and adjusting pH to 7.4  
165 with HCl (aq). The metal solutions (50 mM (final concentration 5 mM), 100 mM (final concentration 10  
166 mM), 200 mM (final concentration 20 mM), and 400 mM (final concentration 40 mM)) were prepared by  
167 dissolving ZnSO<sub>4</sub>, MgSO<sub>4</sub>, MnSO<sub>4</sub>, CuSO<sub>4</sub>, FeSO<sub>4</sub>, NiCl<sub>2</sub>, CoCl<sub>2</sub>, or CaCl<sub>2</sub> in distilled water. PBS (350  
168  $\mu$ L), the purified *FBVMO* (100  $\mu$ L, 1 U/mL in sodium phosphate buffer (50 mM, pH 7.4)), and metal  
169 solution (50  $\mu$ L) were mixed by gently turning it upside down, and incubated at 4 °C for 8 h. The solution  
170 was centrifuged at 4 °C and 5,000 G for 5 min. The precipitant was suspended in PBS and centrifuged at  
171 4 °C and 5,000 G for 5 min twice, and suspended in PBS, giving immobilized *FBVMO* nanocrystal  
172 solution (500  $\mu$ L). The residual protein concentration in the supernatant was determined by the Bradford  
173 method (Bradford 1976), and the immobilization yield was calculated using equation (1).

174

$$\text{Immobilization yield (\%)} = \frac{[\text{Protein}]_I - [\text{Protein}]_R}{[\text{Protein}]_I} \times 100 \quad (1)$$

175

176  $[\text{Protein}]_I$  = Initial protein concentration (mg/mL)

177  $[\text{Protein}]_R$  = Concentration of protein in the supernatant after the *FBVMO* nanocrystal formation and  
178 centrifugation (mg/mL)

179

180 **Scanning Electron Microscope (SEM) analysis of immobilized *FBVMO* nanocrystal**

181 *FBVMO* nanocrystal was analyzed by SEM with a similar method reported in our previous  
182 study (T.sriwong et al. 2020, 2021b). The *FBVMO* nanocrystal was washed with distilled water several  
183 times before being dried at room temperature.

184

185 **Activity measurement of the immobilized enzyme**

186 Cyclohexanone solution (10  $\mu$ L, 0.1 M solution with 10 % diethylene glycol (final  
187 concentration 1 mM)) and sodium phosphate buffer (928  $\mu$ L, pH 7.4, 50 mM) were mixed, and then  
188 NADPH solution (12  $\mu$ L, 10 mg/mL), and immobilized *FBVMO* solution (50  $\mu$ L) were added. Initial

189 velocity was determined by following NADPH consumption at 340 nm for 3 min. Activity assays were  
190 done at 40 °C in duplicate in a 1.0 mL scale.

191

## 192 **Characterization of free and immobilized FBVMO**

193 Effects of pH and on their activities were investigated at 25 °C using 50 mM MES-NaOH  
194 buffer (pH 5, 6), 50 mM sodium phosphate buffer (pH 7, 7.5, 8), 50 mM Tris-HCl buffer (pH 8, 8.5, 9), or  
195 50 mM Glyc-NaOH buffer (pH 9, 10) with the methods described above. For pH 8 and 9, the averages of  
196 the activities in the two buffers are shown. Effects of temperature on their activity were investigated using  
197 sodium phosphate buffer (50 mM, pH 8.0) with the methods described above. Thermostabilities of free  
198 and immobilized FBVMO were investigated by incubating at 40 °C and collecting the portion of the  
199 enzymes at 0, 5, 10, 20, 30, 60, 120, and 300 min for activity measurement described above.

200

## 201 **Preparative-scale oxidation of cyclohexanone by the immobilized FBVMO**

202 FBVMO nanocrystal solution (1 mL) prepared from 1 U of free FBVMO, heat treated  
203 *Thermoplasma acidophilum* glucose dehydrogenase solution (1 mL, 1.95 U) prepared as reported  
204 previously (Are et al. 2021), cyclohexanone solution dissolving 100 mg of cyclohexane in 1 mL of  
205 aqueous solution containing 10% of diethylene glycol, NADPH (50 mg), glucose solution (1 mL of 1 M  
206 solution), and sodium phosphate buffer (17 mL, 50 mM, pH 8.0) were mixed and incubated at 40 °C at  
207 150 rpm for 3 days. The reaction was repeated 5 times to convert 500 mg (5.09 mmol) of cyclohexanone  
208 in total. The reaction mixtures were combined, and the product was extracted with diethyl ether (25 mL x  
209 3), dried over MgSO<sub>4</sub>, evaporated under reduced pressure, purified by silica gel column chromatography  
210 (hexane : ethyl acetate = 3:1), and characterized by <sup>1</sup>H-NMR analysis using CDCl<sub>3</sub> as a solvent. The <sup>1</sup>H-  
211 NMR spectrum was in agreement with that in literature (Omura et al. 2009). Yield 27 % (157 mg, 1.37  
212 mmol). <sup>1</sup>H-NMR (400 MHz, CDCl<sub>3</sub>): δ 1.65-1.87 (6H, m), 2.55-2.65 (2H, m), 4.19 (2H, t, *J* = 4.7Hz).

213

## 214 **Result and Discussion**

### 215 **Screening, overexpression, and purification of FBVMO**

216 Environmental samples from soil, river, and ponds were collected and cultivated using acetone  
217 (50-300 mM) as the only carbon source. Out of 300 samples, two microorganisms were able to grow with  
218 acetone as the only carbon. They were identified as *Fusarium* sp. and *Fusarium oxysporum* Schltdl based  
219 on morphological tests (Supplementary Fig. 1) and ITS-5.8S rDNA sequencing. Encouraged by the  
220 literature search showing the whole cell catalyzed BVO of 2-methylcyclohexanone by *Fusarium* sp. AP-2  
221 (Kawamoto et al. 2008) and the whole-cell catalyzed BVO of alkyl-substituted hexanones by *Fusarium*  
222 *oxysporum* and *Fusarium avenaceum* (Ratu et al. 2009), we examined the presence of BVMO in the  
223 newly isolated *Fusarium* sp. and *F. oxysporum* Schltdl. Cyclohexanone was used as a substrate for the  
224 whole-cell reactions. ε-Caprolactone was successfully obtained in both reactions, suggesting the presence  
225 of a BVMO in both species. *Fusarium* sp. has higher activity than *F. oxysporum* Schltdl, so that *Fusarium*  
226 sp. was deposited to the National Institute of Technology and Evaluation (Tokyo, Japan) as *Fusarium* sp.

227 NBRC 109816, and used for further study.

228 For the use as an efficient biocatalyst, it is necessary to express BVMO from *Fusarium* sp.  
229 NBRC 109816 (*FBVMO*), heterogeneously. Therefore, the gene encoding *FBVMO* was identified,  
230 amplified, and cloned in an expression vector, pET-21b (+), after the removal of the intron, leading to  
231 pET-21b (+)-*FBVMO*. The vector was transformed into *E. coli* BL21(DE3). His-tagged *FBVMO* was  
232 induced by IPTG and purified by Ni affinity chromatography by 17.4 fold in 41% yield (Supplementary  
233 Table 2). The DNA sequence and amino acid sequence are shown in Supplementary Figs. 2 and 3,  
234 respectively. In the deduced amino acid sequences, type I BVMO fingerprint FxGxxxHTxxW[P/D]  
235 (Fraaije et al. 2002; Rebehmed et al. 2013) and [A/G]GxWxxxx[F/Y]P[G/M]xxxD (Riebel et al. 2012)  
236 and two Rossmann fold domains with a GxGxx[G/A] motif were found.

237

### 238 **Immobilization of *FBVMO* and morphology study**

239 To improve the stability, *FBVMO* was immobilized by the organic-inorganic nanocrystal  
240 formation method according to our previous report (T.sriwong et al. 2020, 2021b). The purified *FBVMO*  
241 was mixed with a metal solution to give a catalytically active protein-inorganic nanocrystal. The kind and  
242 the concentration of the metal ion were optimized by investigating 5 mM, 10 mM, 20 mM, and 40 mM of  
243 Zn<sup>2+</sup>, Mg<sup>2+</sup>, Mn<sup>2+</sup>, Cu<sup>2+</sup>, Fe<sup>2+</sup>, Ni<sup>2+</sup>, Co<sup>2+</sup>, and Ca<sup>2+</sup>. The activity of these nanocrystals toward the Baeyer-  
244 Villiger oxidation of cyclohexanone is shown in Fig. 2. Nanocrystal formed using 10 mM of Ca<sup>2+</sup> showed  
245 the best activity among those tested, while high activity was observed in the nanocrystals from most of  
246 the ions except Mn<sup>2+</sup>.

247 Next, the stability of the nanocrystals formed under the optimum concentrations for each metal  
248 was investigated. The nanocrystals used for the activity assay were recovered by centrifugation as a  
249 precipitate, re-suspended in a buffer, and used for the activity assays (Fig 3(a)). To quantify the leakage of  
250 the protein from the nanocrystal, the protein concentration in the supernatant was measured. The amount  
251 of protein retained in the nanocrystal (immobilization yield) is shown in Fig 3(b). It was found that the  
252 *FBVMO* nanocrystal could be recycled up to 8 times with retained activity. The remaining activity after  
253 recycling largely depends on the kind of metal ions used for immobilization. The activity of the 10 mM  
254 Ca<sup>2+</sup> nanocrystal, showing the best activity for the 1<sup>st</sup> usage, decreased dramatically by recycling, and its  
255 protein leakage was also obvious. On the other hand, while the activity of 20 mM Cu<sup>2+</sup> nanocrystal was  
256 moderate for the 1<sup>st</sup> usage (52%), it did not decrease significantly for the 8<sup>th</sup> usage (42%), so as for the  
257 immobilization yield being 69% for the 1<sup>st</sup> usage and 53% for the 8<sup>th</sup> usage. Therefore, the best metal ion  
258 and its optimum concentration were determined to be Cu<sup>2+</sup> and 20 mM.

259 The morphology study of *FBVMO*-Cu<sup>2+</sup> nanocrystal was conducted by SEM analysis  
260 (Supplementary Fig. 4). We found that the *FBVMO*-Cu<sup>2+</sup> nanocrystal forms a porous structure  
261 (Supplementary Fig. 4(b)), which could not be seen in the control copper (II) phosphate crystal without  
262 the enzyme (Supplementary Fig. 4 (a)). The high porosity of the sponge-like structure may cause the high  
263 activity of the *FBVMO*-Cu<sup>2+</sup> nanocrystal.

264

## 265 **Characterization of free and immobilized FBVMO**

266 First, the effect of pH on the activity of the free and immobilized *FBVMO* toward the  
267 oxidation of cyclohexanone was investigated. As shown in Fig. 4(a), similar results were obtained for the  
268 free and immobilized enzyme, showing the highest activity around pH 8.0 - 8.5. Next, the effect of  
269 temperature on the activity of the free and immobilized *FBVMO* toward the oxidation of cyclohexanone  
270 was investigated. As shown in Fig. 4(b), the optimum temperature for the free and immobilized *FBVMO*  
271 were 30 °C and 40 °C, respectively. The activity at 40 °C increased significantly by immobilization. The  
272 free enzyme activity at 40 °C was 1.27 nmol·min<sup>-1</sup>·mg<sup>-1</sup> protein, while the immobilized enzyme activity at  
273 40 °C was 15.3 nmol·min<sup>-1</sup>·mg<sup>-1</sup> protein. The immobilization improved the activity at 40 °C by 12 times.  
274 Then, the thermostability of the free and immobilized *FBVMO* was investigated. As shown in Fig. 4(c),  
275 the free *FBVMO* had only 18% of the remaining activity after incubation for 5 min at 40 °C, while >90%  
276 of the activity of the immobilized *FBVMO* was retained after 5 h at 40 °C. The thermostability of the  
277 *FBVMO* was significantly improved by immobilization. The nanocrystal formation method was proven  
278 as a promising approach for BVMOs immobilization. The confinement of enzymes in the nanocrystal  
279 may have fixed the unstable residue of the protein, as support materials act as a shell to protect the  
280 enzyme from harsh environments, including high temperatures in general immobilization methods (Hu et  
281 al. 2018; T.sriwong et al. 2021b). The successful result of immobilization of *FBVMO*, improving the  
282 thermostability, is remarkable since there are only a few examples (Cassimjee et al. 2014; Delgove et al.  
283 2019) for the immobilization of BVMOs due to the low stability of BVMOs.

284 Substrate specificities of the free and immobilized *FBVMO* were investigated using varieties  
285 of ketones and sulfides. Both of the free and immobilized *FBVMO* successfully oxidized a wide range of  
286 ketones (Table 1, Entries 1-8), and sulfides (Table 1, Entries 9-13). In general, it was clear that the broad  
287 substrate specificity of the free *FBVMO* was greatly retained after immobilization. However, the  
288 difference in the relative activities between the free and immobilized *FBVMO* were also seen for the  
289 bulky substrates. The free enzyme exhibited about 3-5 times higher activities for cyclooctanone, 2-  
290 pentylcyclopentan-1-one, 4-phenylbutan-2-one, and diphenyl sulfide (Table 1, Entries 3, 4, 8, 13). The  
291 change in the substrate preference by the immobilization is an intriguing phenomenon, since it was not  
292 observed for the case of other enzymes such as *Geotrichum candidum* aldehyde dehydrogenase  
293 (T.sriwong et al. 2021b). This might be caused by the subtle structural change of the enzyme by the  
294 immobilization or by the restriction in the substrate transfer to the active site of the immobilized enzyme  
295 due to the diminished flexibility of the residue at the entrance caused by the metal shell.

296 At last, a preparative scale reaction by the immobilized *FBVMO* was conducted using  
297 cyclohexanone as a substrate. The reaction proceeded smoothly, and the product was successfully  
298 isolated, purified, and identified by the <sup>1</sup>H NMR (Supplementary Fig. 5).

299

## 300 **Conclusion**

301 *FBVMO* was discovered from an environmental sample by the screening of microorganisms  
302 using acetone as the only carbon source. *FBVMO* was successfully immobilized by the organic-inorganic



303 nanocrystal formation method, resulting in an improvement in thermostability. Both free and immobilized  
304 enzymes were characterized, and found to be versatile for both BVO and oxidation of sulfide. At last,  
305 preparative scale reaction of BVO of cyclohexane was successfully conducted.

306

#### 307 **Author contributions**

308 M.T. and K.T. contributed equally to this work.

309

#### 310 **Acknowledgement**

311 We would like to acknowledge Prof. Nobuo Nomura from Department of Human Sciences,  
312 Faculty of Human Sciences, Musashino University, Tokyo, Japan for the discussion regarding the  
313 isolation of *FBVMO* gene and overexpression, and Hiroumi Nemoto, Haruka Maeda, Tomofumi Tanabe,  
314 Ayana Hirukawa, Muhammad Maulana Ichsan from our laboratory for the related research. The authors  
315 are grateful to TechnoSuruga Laboratory Co., Ltd. Japan for the identification and examination of the  
316 microorganism. This work was supported by the Japan Society for the Promotion of Science (JSPS,  
317 KAKENHI Grant Number JP19K05560).

318

#### 319 **References**

- 320 Altinkaynak C, Yilmaz I, Koksal Z, et al (2016) Preparation of lactoperoxidase incorporated hybrid  
321 nanoflower and its excellent activity and stability. *Int J Biol Macromol* 84:402–409.  
322 <https://doi.org/https://doi.org/10.1016/j.ijbiomac.2015.12.018>
- 323 Are KRA, Ohshima S, Koike Y, et al (2021) Enzymatic direct carboxylation under supercritical CO<sub>2</sub>.  
324 *Biochem Eng J* 171:108004. <https://doi.org/https://doi.org/10.1016/j.bej.2021.108004>
- 325 Basso A, Serban S (2019) Industrial applications of immobilized enzymes—A review. *Mol Catal*  
326 479:110607. <https://doi.org/https://doi.org/10.1016/j.mcat.2019.110607>
- 327 Birolli WG, Lima RN, Porto ALM (2019) Applications of marine-derived microorganisms and their  
328 enzymes in biocatalysis and biotransformation, the underexplored potentials. *Front Microbiol* 10:.  
329 <https://doi.org/10.3389/fmicb.2019.01453>
- 330 Bong YK, Song S, Nazor J, et al (2018) Baeyer-Villiger Monooxygenase-Mediated Synthesis of  
331 Esomeprazole As an Alternative for Kagan Sulfoxidation. *J Org Chem* 83:7453–7458.  
332 <https://doi.org/10.1021/acs.joc.8b00468>
- 333 Bradford MM (1976) A Rapid and Sensitive Method for the Quantitation Microgram Quantities of  
334 Protein Utilizing the Principle of Protein-Dye Binding. 254:248–254
- 335 Bryliakov KP (2017) Catalytic Asymmetric Oxygenations with the Environmentally Benign Oxidants  
336 H<sub>2</sub>O<sub>2</sub> and O<sub>2</sub>. *Chem Rev* 117:11406–11459. <https://doi.org/10.1021/acs.chemrev.7b00167>
- 337 Cassimjee KE, Kadow M, Wikmark Y, et al (2014) A general protein purification and immobilization

338 method on controlled porosity glass: biocatalytic applications. *Chem Commun* 50:9134–9137.  
339 <https://doi.org/10.1039/c4cc02605e>

340 Chen YC, Peoples OP, Walsh CT (1988) *Acinetobacter* cyclohexanone monooxygenase: gene cloning  
341 and sequence determination. *J Bacteriol* 170:781–789. [https://doi.org/10.1128/jb.170.2.781-](https://doi.org/10.1128/jb.170.2.781-789.1988)  
342 789.1988

343 Delgove MAF, Valencia D, Solé J, et al (2019) High performing immobilized Baeyer-Villiger  
344 monooxygenase and glucose dehydrogenase for the synthesis of  $\epsilon$ -caprolactone derivative. *Appl*  
345 *Catal A Gen* 572:134–141. <https://doi.org/10.1016/j.apcata.2018.12.036>

346 Dong JJ, Fernández-Fueyo E, Hollmann F, et al (2018) Biocatalytic Oxidation Reactions: A Chemist's  
347 Perspective. *Angew Chemie - Int Ed* 57:9238–9261. <https://doi.org/10.1002/anie.201800343>

348 Donoghue NA, Norris DB, Trudgill PW (1976) The Purification and Properties of Cyclohexanone  
349 Oxygenase from *Nocardia globerula* CL1 and *Acinetobacter* NCIB 9871. *Eur J Biochem* 63:175–  
350 192. <https://doi.org/10.1111/j.1432-1033.1976.tb10220.x>

351 Fordwour OB, Luka G, Hoorfar M, Wolthers KR (2018) Kinetic characterization of acetone  
352 monooxygenase from *Gordonia* sp. strain TY-5. *AMB Express* 8:1–13.  
353 <https://doi.org/10.1186/s13568-018-0709-x>

354 Fraaije MW, Kamerbeek NM, van Berkel WJH, Janssen DB (2002) Identification of a Baeyer-Villiger  
355 monooxygenase sequence motif. *FEBS Lett* 518:43–47. [https://doi.org/10.1016/s0014-](https://doi.org/10.1016/s0014-5793(02)02623-6)  
356 5793(02)02623-6

357 Franceschini S, Van Beek HL, Pennetta A, et al (2012) Exploring the structural basis of substrate  
358 preferences in Baeyer-Villiger monooxygenases: Insight from steroid monooxygenase. *J Biol Chem*  
359 287:22626–22634. <https://doi.org/10.1074/jbc.M112.372177>

360 Fürst MJLJ, Gran-Scheuch A, Aalbers FS, Fraaije MW (2019) Baeyer-Villiger Monooxygenases:  
361 Tunable Oxidative Biocatalysts. *ACS Catal* 9:11207–11241.  
362 <https://doi.org/10.1021/acscatal.9b03396>

363 Fürst MJLJ, Savino S, Dudek HM, et al (2017) Polycyclic ketone monooxygenase from the thermophilic  
364 fungus *Thermothelomyces thermophila*: A structurally distinct biocatalyst for bulky substrates. *J*  
365 *Am Chem Soc* 139:627–630. <https://doi.org/10.1021/jacs.6b12246>

366 Ge J, Lei J, Zare RN (2012) Protein-inorganic hybrid nanoflowers. *Nat Nanotechnol* 7:428–432.  
367 <https://doi.org/10.1038/nnano.2012.80>

368 Hausinger RP (2007) New insights into acetone metabolism. *J Bacteriol* 189:671–673.  
369 <https://doi.org/10.1128/JB.01578-06>

370 Hu Y, Dai L, Liu D, et al (2018) Progress & prospect of metal-organic frameworks (MOFs) for enzyme

371 immobilization (enzyme/MOFs). *Renew Sustain Energy Rev* 91:793–801.  
372 <https://doi.org/10.1016/j.rser.2018.04.103>

373 Kawamoto M, Utsukihara T, Abe C, et al (2008) Biotransformation of ( $\pm$ )-2-methylcyclohexanone by  
374 fungi. *Biotechnol Lett* 30:1655–1660. <https://doi.org/10.1007/s10529-008-9729-y>

375 Know GR (1993) The Baeyer-Villiger oxidation of ketones and aldehydes. In: Paquette LA (ed) *Organic*  
376 *reactions*. John Wiley & Sons, Inc, pp 251–798

377 Koesoema AA, Standley DM, Senda T, Matsuda T (2020) Impact and relevance of alcohol  
378 dehydrogenase enantioselectivities on biotechnological applications. *Appl. Microbiol. Biotechnol.*  
379 *104*:2897–2909

380 Kyte BG, Rouvière P, Cheng Q, Stewart JD (2004) Assessing the Substrate Selectivities and  
381 Enantioselectivities of Eight Novel Baeyer-Villiger Monooxygenases toward Alkyl-Substituted  
382 Cyclohexanones. *J Org Chem* 69:12–17. <https://doi.org/10.1021/jo0302531>

383 Leipold F, Rudroff F, Mihovilovic MD, Bornscheuer UT (2013) The steroid monooxygenase from  
384 *Rhodococcus rhodochrous*; A versatile biocatalyst. *Tetrahedron Asymmetry* 24:1620–1624.  
385 <https://doi.org/10.1016/j.tetasy.2013.11.003>

386 Leipold F, Wardenga R, Bornscheuer UT (2012) Cloning, expression and characterization of a eukaryotic  
387 cycloalkanone monooxygenase from *Cylindrocarpus radialis* ATCC 11011. *Appl Microbiol*  
388 *Biotechnol* 94:705–717. <https://doi.org/10.1007/s00253-011-3670-z>

389 Liese A, Hilterhaus L (2013) Evaluation of immobilized enzymes for industrial applications. *Chem Soc*  
390 *Rev* 42:6236–6249. <https://doi.org/10.1039/C3CS35511J>

391 Liu C, Wen KG, Zeng XP, Peng YY (2020) Advances in Chemocatalytic Asymmetric Baeyer–Villiger  
392 Oxidations. *Adv Synth Catal* 362:1015–1031. <https://doi.org/10.1002/adsc.201901178>

393 López-Gallego F, Yate L (2015) Selective biomineralization of  $\text{Co}_3(\text{PO}_4)_2$ -sponges triggered by His-  
394 tagged proteins: efficient heterogeneous biocatalysts for redox processes. *Chem Commun* 51:8753–  
395 8756. <https://doi.org/10.1039/C5CC00318K>

396 Matsuda T (ed) (2017) *Future directions in biocatalysis*, 2nd editio. Elsevier, Amsterdam

397 Mohamad NR, Marzuki NHC, Buang NA, et al (2015) An overview of technologies for immobilization  
398 of enzymes and surface analysis techniques for immobilized enzymes. *Biotechnol Biotechnol Equip*  
399 *29*:205–220. <https://doi.org/10.1080/13102818.2015.1008192>

400 Morii S, Sawamoto S, Yamauchi Y, et al (1999) Steroid monooxygenase of *Rhodococcus rhodochrous*:  
401 Sequencing of the genomic DNA, and hyperexpression, purification, and characterization of the  
402 recombinant enzyme. *J Biochem* 126:624–631.  
403 <https://doi.org/10.1093/oxfordjournals.jbchem.a022494>

404 Nguyen Q-T, Mattevi A, Fraaije MW (2017) Chapter 6 - Expanding the Repertoire of Flavoenzyme-  
405 Based Biocatalysis. In: Matsuda T (ed) Future Directions in Biocatalysis (Second Edition). Elsevier,  
406 Amsterdam, pp 119–133

407 Omura S, Fukuyama T, Murakami Y, et al (2009) Hydro-ruthenation triggered catalytic conversion of  
408 dialdehydes and keto aldehydes to lactones. *Chem Commun* 6741–6743.  
409 <https://doi.org/10.1039/B912850F>

410 Ratu B, Gładkowski W, Wawrze C (2009) Enzyme and Microbial Technology New aspects of the  
411 application of *Fusarium* strains to production of. 45:156–163.  
412 <https://doi.org/10.1016/j.enzmictec.2009.04.008>

413 Rebehmed J, Alphan V, de Berardinis V, de Brevern AG (2013) Evolution study of the Baeyer-Villiger  
414 monooxygenases enzyme family: functional importance of the highly conserved residues.  
415 *Biochimie* 95:1394–1402. <https://doi.org/10.1016/j.biochi.2013.03.005>

416 Rehdorf J, Kirschner A, Bornscheuer UT (2007) Cloning, expression and characterization of a Baeyer-  
417 Villiger monooxygenase from *Pseudomonas putida* KT2440. *Biotechnol Lett* 29:1393–1398.  
418 <https://doi.org/10.1007/s10529-007-9401-y>

419 Riebel A, Dudek HM, De Gonzalo G, et al (2012) Expanding the set of rhodococcal Baeyer-Villiger  
420 monooxygenases by high-throughput cloning, expression and substrate screening. *Appl Microbiol*  
421 *Biotechnol* 95:1479–1489. <https://doi.org/10.1007/s00253-011-3823-0>

422 Sheldon RA, Woodley JM (2018) Role of Biocatalysis in Sustainable Chemistry. *Chem Rev* 118:801–  
423 838. <https://doi.org/10.1021/acs.chemrev.7b00203>

424 T.sriwong K, Kamogawa R, Issasi CSC, et al (2021a) *Geotrichum candidum* acetophenone reductase  
425 immobilization on reduced graphene oxide: a promising biocatalyst for green asymmetric reduction  
426 of ketones. *Biochem Eng J* 108263. <https://doi.org/10.1016/j.bej.2021.108263>

427 T.sriwong K, Koesoema AA, Matsuda T (2020) Organic-inorganic nanocrystal reductase to promote  
428 green asymmetric synthesis. *RSC Adv* 10:30953–30960. <https://doi.org/10.1039/d0ra03160g>

429 T.sriwong K, Ogura K, Hawari MA, Matsuda T (2021b) *Geotrichum candidum* aldehyde dehydrogenase-  
430 inorganic nanocrystal with enhanced activity. *Enzyme Microb Technol* 150:109866.  
431 <https://doi.org/10.1016/j.enzmictec.2021.109866>

432 Wiegant WM, De Bont JAM (1980) A new route for ethylene glycol metabolism in *Mycobacterium* E44.  
433 *J Gen Microbiol* 120:325–331. <https://doi.org/10.1099/00221287-120-2-325>

434 Woo JM, Jeon EY, Seo EJ, et al (2018) Improving catalytic activity of the Baeyer-Villiger  
435 monooxygenase-based *Escherichia coli* biocatalysts for the overproduction of (Z)-11-  
436 (heptanoyloxy)undec-9-enoic acid from ricinoleic acid. *Sci Rep* 8:1–11.

437 <https://doi.org/10.1038/s41598-018-28575-8>  
438 Wu S, Snajdrova R, Moore JC, et al (2020) Biocatalysis: Enzymatic Synthesis for Industrial Applications.  
439 Angew Chemie - Int Ed 2–34. <https://doi.org/10.1002/anie.202006648>  
440 Yin Y, Xiao Y, Lin G, et al (2015) An enzyme-inorganic hybrid nanoflower based immobilized enzyme  
441 reactor with enhanced enzymatic activity. J Mater Chem B 3:2295–2300.  
442 <https://doi.org/10.1039/c4tb01697a>  
443 Yu Y, Fei X, Tian J, et al (2015) Self-assembled enzyme–inorganic hybrid nanoflowers and their  
444 application to enzyme purification. Colloids Surfaces B Biointerfaces 130:299–304.  
445 <https://doi.org/https://doi.org/10.1016/j.colsurfb.2015.04.033>  
446 Zhang Y, Sun W, Elfeky NM, et al (2020) Self-assembly of lipase hybrid nanoflowers with bifunctional  
447 Ca<sup>2+</sup> for improved activity and stability. Enzyme Microb Technol 132:109408.  
448 <https://doi.org/https://doi.org/10.1016/j.enzmictec.2019.109408>

449  
450

#### 451 **Supporting information**

452 Reagents, materials, and apparatus

453 **Table 1** Primers used for PCR to construct BL21(DE3)-pET-21b(+)-FBVMO

454 **Table 2** Summary of purification steps of FBVMO overexpressed in *E. coli*

455 **Fig. 1** Microscopic observation images of *Fusarium* sp. NBRC 109816

456 **Fig. 2** DNA sequence of FBVMO without intron

457 **Fig. 3** Amino acid sequence of FBVMO

458 **Fig. 4** SEM images of crystals formed by mixing PBS and CuSO<sub>4</sub> solution (a) without and (b) with  
459 FBVMO

460 **Fig. 5** <sup>1</sup>H NMR spectrum of ε-caprolactone obtained by oxidation of cyclohexanone with immobilized  
461 FBVMO

462

#### 463 **Conflict of interest**

464 The authors declare that they have no conflict of interest.

#### 465 **Figure legends**

466 **Fig. 1** Baeyer–Villiger monooxygenase (BVMO) catalyzed reaction

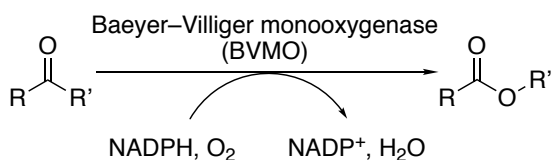
467 **Fig. 2** Effect of kind and concentration of metal ions for immobilization on residual activity. Activity  
468 before immobilization was set to 100%. The activity was determined at 40 °C, pH 7.4.

469 **Fig. 3** Effect of recycling of immobilized FBVMO on (a) activity and (b) immobilization yield The

470 activity was determined at 40 °C at pH 7.4. The optimum metal ion concentrations determined in  
 471 Fig. 1 was employed. Activity before immobilization was set to 100%. Protein concentration before  
 472 immobilization was set to 100%.

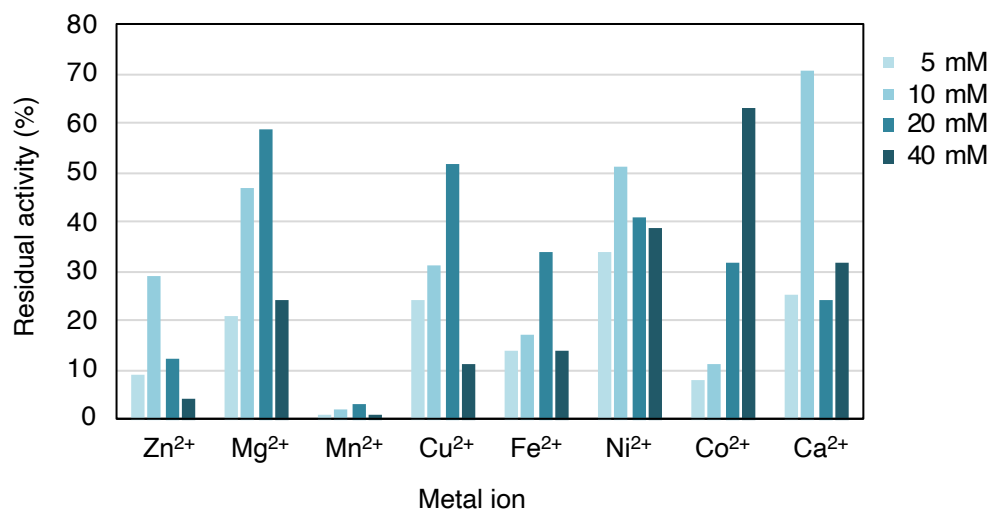
473 **Fig. 4** Effect of (a) pH and (b) temperature on oxidation activity of *FBVMO*, and (c) thermo-stability of  
 474 *FBVMO* at 40 °C. Closed blue circle: immobilized *FBVMO*, open red circle: free *FBVMO* (a)  
 475 Activity at pH 8.0 was set to 100% for free enzymes, and activity at pH 8.5 was set to 100% for  
 476 immobilized *FBVMO*. (b) Activity at 30 °C was set to 100% (0.0192  $\mu\text{mol}\cdot\text{min}^{-1}\cdot\text{mg}^{-1}$  protein) for  
 477 free enzymes, and activity at 40 °C was set to 100% (0.0153  $\mu\text{mol}\cdot\text{min}^{-1}\cdot\text{mg}^{-1}$  protein) for  
 478 immobilized *FBVMO*. (c) The activities before the treatment were set to 100%.

479  
 480  
 481  
 482



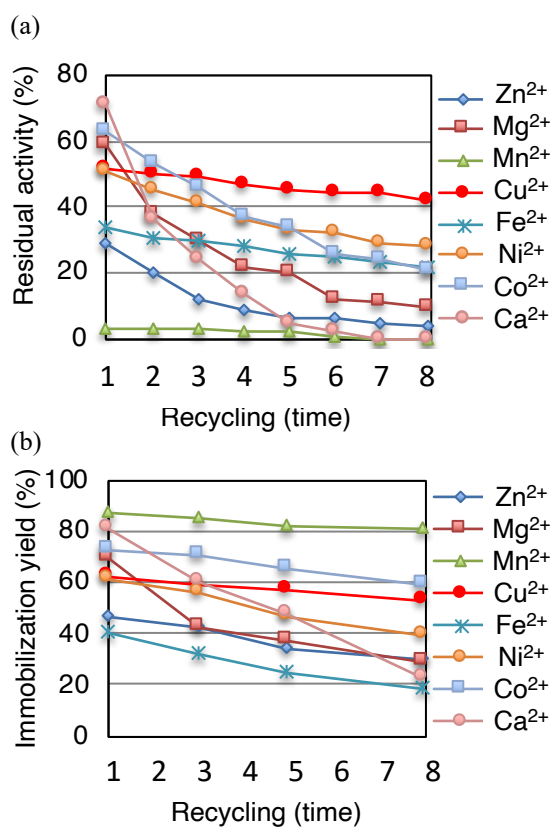
483  
 484  
 485  
 486  
 487

**Fig. 1** Baeyer-Villiger monooxygenase (BVMO) catalyzed reaction

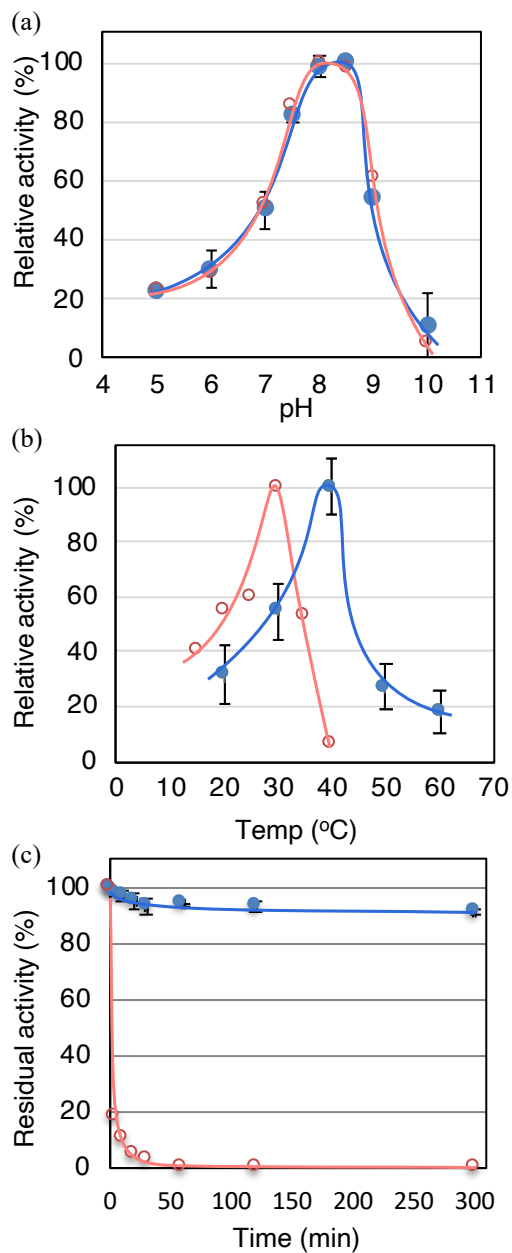


488  
 489  
 490

**Fig. 2** Effect of kind and concentration of metal ions for immobilization on residual activity. Activity before immobilization was set to 100%. The activity was determined at 40 °C, pH 7.4.



491 **Fig. 3** Effect of recycling of immobilized FBVMO on (a) activity and (b) immobilization yield  
 492 The activity was determined at 40 °C at pH 7.4. The optimum metal ion concentrations determined in Fig.  
 493 1 was used. Activity before immobilization was set to 100%. Protein concentration before immobilization  
 494 was set to 100%.  
 495



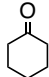
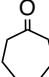
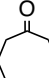
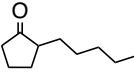
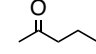
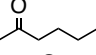
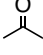
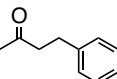
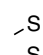
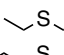
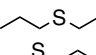
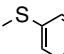
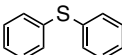
496 **Fig. 4** Effect of (a) pH and (b) temperature on oxidation activity of FBVMO, and (c) thermo-stability of  
 497 FBVMO at 40 °C. Closed blue circle: immobilized FBVMO, open red circle: free FBVMO  
 498 (a) Activity at pH 8.0 was set to 100% for free enzymes, and activity at pH 8.5 was set to 100% for  
 499 immobilized FBVMO.  
 500  
 501 (b) Activity at 30 °C was set to 100% ( $0.0192 \mu\text{mol}\cdot\text{min}^{-1}\cdot\text{mg}^{-1}$  protein) for free enzymes, and activity at  
 502 40 °C was set to 100% ( $0.0153 \mu\text{mol}\cdot\text{min}^{-1}\cdot\text{mg}^{-1}$  protein) for immobilized FBVMO.  
 503 (c) The activities before the treatment were set to 100%.  
 504

505  
 506  
 507  
 508



509

**Table 1** Substrate specificity of *FBVMO*

Entry	Substrate		Relative activity (%)	
			Free <i>FBVMO</i>	Immobilized <i>FBVMO</i>
1	Cyclohexanone		100	100
2	Cycloheptanone		16	18
3	Cyclooctanone		5.1	1.8
4	2-Pentylcyclopentan-1-one		83	18
5	Pentan-2-one		5.1	4.6
6	Heptan-2-one		2.7	2.8
7	1-Cyclopropylethan-1-one		3.0	2.2
8	4-Phenylbutan-2-one		83	18
9	Dimethyl sulfide		2.8	3.2
10	Diethyl sulfide		14	16
11	Dipropyl sulfide		3.2	3.0
12	Methyl phenyl sulfide		29	18
13	Diphenyl sulfide		3.1	0.6

510

The activities were determined under the standard assay conditions at pH 8.0 in 50 mM sodium phosphate buffer at 25 °C for the assay with the free *FBVMO* and 40 °C for the assay with the immobilized *FBVMO*. The activities of free or immobilized *FBVMO* toward cyclohexanone were set to 100%, respectively.

511

512

513

## Supplementary Information

### Immobilization of Baeyer-Villiger monooxygenase from acetone grown *Fusarium* sp.

Michio Takagi, Kotchakorn T.sriwong, Ayaka Masuda, Nozomi Kawaguchi, Shusuke Fukui, Huong Le Viet Lan, Dai-ichiro Kato, Takashi Kitayama, Mikio Fujii, Afifa Ayu Koesoema, Tomoko Matsuda

#### Table of content

Reagents, materials, and apparatus	1
<b>Table 1</b> Primers used for PCR to construct BL21(DE3)-pET-21b(+)-FBVMO	2
<b>Table 2</b> Summary of purification steps of FBVMO overexpressed in <i>E. coli</i>	2
<b>Fig. 1</b> Microscopic observation images of <i>Fusarium</i> sp. NBRC 109816	2
<b>Fig. 2</b> DNA sequence of FBVMO without intron	3
<b>Fig. 3</b> Amino acid sequence of FBVMO	3
<b>Fig. 4</b> SEM images of crystals formed by mixing PBS and CuSO <sub>4</sub> solution (a) without and (b) with FBVMO	4
<b>Fig. 5</b> <sup>1</sup> H NMR spectrum of ε-caprolactone obtained by oxidation of cyclohexanone with immobilized FBVMO	4
References	5

#### Reagents, materials, and apparatus

Chemicals were purchased from Nacalai Tesque (Kyoto, Japan), Tokyo Chemical Industry (Tokyo, Japan), or Wako (Tokyo, Japan) unless otherwise indicated. All reagents were used without purification. Restriction enzymes, DNA marker for Agarose gel electrophoresis, λDNA/HindIII Markers G1711, Pure Yield™ Plasmid Miniprep System, and Wizard SV Gel PCR Clean-Up System were purchased from Promega (USA). Ex Taq polymerase and In-Fusion HD Cloning Kit were purchased from Takara Bio (Shiga, Japan). Precision Plus Protein™ All Blue Standards, and protein concentration measurement reagent (Bradford reagent) were purchased from Bio-rad (USA). GenElute™ Plant Genomic DNA Miniprep Kit and 4-(2-hydroxyethyl)-1-piperazineethanesulfonic acid (HEPES) were purchased from Sigma Aldrich (USA). HisTrap™FF crude (1 mL) was purchased from GE Healthcare (Tokyo, Japan). Amicon Ultra-4 (10 k) was purchased from Merk Millipore (USA).

Experiments were done using Bio-shaker BR-43FL from Taitech (Nagoya, Japan), high speed centrifuge TOMY MX-301 from Tomy Seiko (Tokyo, Japan), Gen Amp PCR system 9700 from Applied Biosystems (USA), and insonator 201 M from Kubota (Tokyo, Japan). Enzyme activity assays were performed on a UV-1900-UV-Vis spectrophotometer from Shimadzu (Kyoto, Japan). GC analysis was performed on a GC-14B equipped with FID detector and CP-Chirasil DEX CB column (Varian, 25 m x 0.32 mm, and 0.25 μm film thickness). <sup>1</sup>H-NMR analysis was performed on a Bruker Biospin AVANCE III 400 spectrometer at 400 MHz in CDCl<sub>3</sub>. Morphological observation was done by Bench-top Scanning Electron Microscope (SEM) proX supplied by Phenom-World (Netherlands).

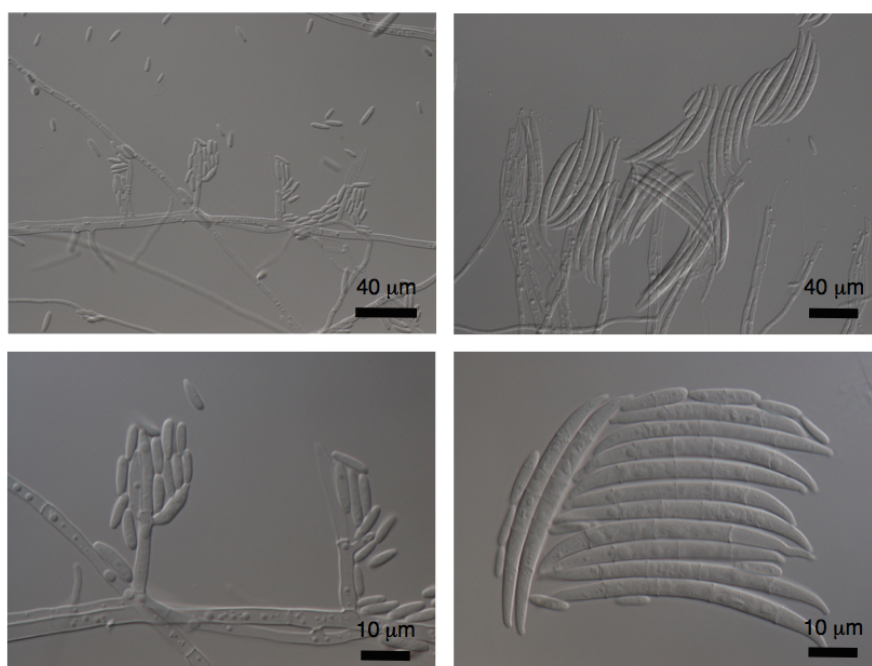
**Table 1** Primers used for PCR to construct BL21(DE3)-pET-21b(+)-FBVMO

Purposes	Sequence
Determination of FBVMO sequence	Forward primer-1 (5'-GCAAAAGGTCCCGAACATAA-3')
	Reverse primer-1 (5'-ATGATGTGATGGCTGTCCAA-3')
	Forward primer-2 (5'-GTGATCTCGGTGATGGGAGT-3')
	Reverse primer-2 (5'-GGAAGCAAGCAAAAGAGAGC-3')
Removal of the intron and construction of pUC19-FBVMO	Forward primer-3 (5'-CTTGCCCCAAGCATGGAC-3')
	Reverse primer-3 (5'-GTCAAGGCCGAGAAGCTGAT-3')
	Forward primer-4 (5'-CATGTCACAGCAATACGGAGA-3')
	Reverse primer-4 (5'-GATATCATCCAACACGCCAAC-3')
Construction of pET-21b(+)-FBVMO	pUC19-BVMO forward primer (5'-TCGGTACCCGGGATCATGACCCCTTGTCTGATTACG-3')
	BVMO intron reverse primer (5'-AACATCGAAGGCGTCTCCGACATGGC-3')
	BVMO intron forward primer (5'-GGATACGCCTTCGATGTT-3')
	pUC19-BVMO reverse primer (5'-TCGACTCTAGAGGATCGTCACTTCAGAACGGTCTAAATCC-3')
Construction of pET-21b(+)-FBVMO	Insert forward primer (5'-AAGGAGATATACATGACCCCTTGTCTGATTACG-3')
	Insert reverse primer (5'-GTCATGCTAGCCATAAACGGTCTAAATCCTTTGTATCC-3')

**Table 2** Summary of purification steps of FBVMO overexpressed in *E. coli*

Step	Total protein (mg)	Total unit (U)	Specific activity (U/mg) <sup>a</sup>	Yield (%)	Purification fold
Cell free extract	1.50	1.91	1.27	100	1
HisTrap FF crude	0.0352	0.78	22.1	41	17.4

<sup>a</sup>The specific activity was measured using 0.1% diethylene glycol to dissolve substrate, cyclohexanone, easily. The specific activity without using diethylene glycol was same as that with diethylene glycol.

**Fig. 1** Microscopic observation images of *Fusarium* sp. NBRC 109816

ATGACCCCTTGCCTGATTACGATGCTGTAGTAGTGGGAGCTGGCTTTGGTGGCATCTACATGT  
 GCAAGAAGCTCGTGGACCAGGGCCTGTCTGTGAAGCTTATCGAGGTTGCGCCGGATGTTGGC  
 GGCACCTTGGTATTGGAATCGTTATCCGGGCGCCATGTCGGATACGCCTTCGATGTTGTATAGAT  
 ACTCTTGGGACCTCGAAGATCTTCAGCAGTATTCATGGGAAAAGCAATACCTCCAACAACATG  
 AGGTTTTGGCTTACCTACGGCATGTGGTTGATCGACATCAACTCCGTCAATATATGCAGTTCAA  
 CGCTGAGATGAAAGCTGCCAACTGGGATCCAGACCACTCAAAATGGACTGTTGGTCTATCTTC  
 TGGTCCGGATACACATGTCGCTACTTGATCACCGCGATTGGGCTTCTTTCCAAGCAGAATTAT  
 CCAGAAATCCGGGGATTGGATTCTTCAAGGGCGAAAATGTATCACACAGGGAGCTGGCCAGC  
 GTCTTACGACTTCAAGAATAAGCGAGTCCGGGTTATTGGGAACGGATCGACCGGTGTTCAAG  
 TCATTACCGCAATGTCAGATGAAGTAAAGCTTCTGCGTTCATTCCAGCGGCACCCCGCAGTATG  
 TTGTGCCTGCAGTCAATAGAGCGTTTCTCCTGAAGATCGACGCGAGATTGACCGCCAATGGA  
 ACGAGATCTGGAAGCAAGCAAAAGAGAGCATGTTTGGTTTTGGATTTCGAGGAGAGTCAAAC  
 CCTGCCTATAGTGTACAGCAGAAGAGCGTGAAAAGATCTTCGAGAACGCCTGGCAAAAGG  
 GTGGCGGCTTCAACTTTATGTTTCGGAACCTTTCCGACATCTCTTCTGACGAAGCGGCAAAACA  
 AAGAAGCAGCCGACTTTATCAAAAGAAAGATCCGCCAAATCGTCAAAGATCCTATCAAGGCC  
 GAGAAGCTGATTCCCACAGAGCATTATGCTCGTCCACTGTGTGATACGGGTTATTATGAG  
 AAGTTCAACAGCCATAATGTGGATATCATTGATGTCAATGAGACTCCCATCACCGAGATCACG  
 CCTAAGGGTGTTCGAACAAGCGACGGGGCGAGTATGACCTCGATGTTCTTGTGTTTGCCAC  
 AGGTTTTGATGCCGTAGATGGGAACAAGCGGATTCCGATCCAAGGTGTATCAAACAAGAC  
 TCTCAAGGACTGTTGGGCTGATGGACCAGACTCATATCTCGGTATCTCTGTATCAGACTTCCCA  
 AATCTCTTCATGATACTGGGTCCGAACGGTCTTTTACAAATTTGCCCCGACCATTGAGACCC  
 AGGTTGAGTTTGTATCTGACATCCTCAACACGCCAATGAATCGGCACGTCAGAACGGCAAG  
 AATCCTACTATTGAAGCAGAGCGAGAAGCGGTCCATGCTTGGAGCAAGATCTGTGACGAGCT  
 TAGCGCAAACAGTTTATTAGAAGGACAGATTCTTGGATTTTTGGTGCTAACGTAGCTGGGAA  
 AAAGCCTTCGGTGTCTTTTACTTTGGAGGTCTTGCAAACATATAGGAAGGCCTTGCAGGATTT  
 GATCGATGATGGATACAAAGGATTTAGACCGTTATGGCTAGCATGACTGGTGGACAGCAAAT  
GGGTCGGGGATCCGAATTCGAGCTCCGTCGACAAGCTTGCGGCCGCACTCGAGACCACCAC  
 CACCACCAC

**Fig. 2** DNA sequence of *FBVMO* without intron  
 green: sequence of *FBVMO*,  
 yellow: sequence of restriction enzyme site,  
 blue: sequence of His Tag,  
 under line: sequence of T7 · Tag

MTPCPDYDAVVVGAGFGGIYMCKKLVDQGLSVKLIEVAPDVGGTWYWNRYPGAMSDTPSML  
 YRYSWDLEDLQQYSWEKQYLQQHEVLAYLRHVVDHRQLRQYMQFNAEMKAANWDPDHSKW  
 TVGLSSGPDITCRYLITAIGLLSKQNYPEIRGLDSFKGEMYHTGSWPASYDFKNKRVGVINGST  
GVQVITAIADDEVKLLRSFQRHPQYVVPVAVNRAFPPEDRREIDRQWNEIWKQAKESMFGFGFEES  
 QTPAYSVTAEREKIFENAWQKGGGFNFMFGTFSDISSDEAANKEAADFIKIRKIRQIVKDKPIAEK  
 LIPTEHYARRPLCDTGYEKFNSHNVDIIDVNETPITEITPKGVRTSDGAEYDLVLFVATGFDAV  
 DGNYKRIPIQGVSNKTLKDCWADGPDSYLGISVSDFPNLFMILGPNGPFTNLPPTIETQVEFVSDII  
 QHANESARQNGKNPTIEAEREAVHAWSKICDELSANSLFRRTDSWIFGANVAGKKPSVLFYFGG  
 LANYRKALQDLIDDGYKGFRPF\*

**Fig. 3** Amino acid sequence of *FBVMO*  
 blue: type I BVMO fingerprint; FxGxxxHTxxW[P/D] (Fraaije et al. 2002; Rebehmed et al. 2013)  
 green: type I BVMO fingerprint; [A/G]GxWxxxx[F/Y]P[G/M]xxxD (Riebel et al. 2012)  
 red: two Rossmann fold domains harboring a GxGxx [G/A] motif

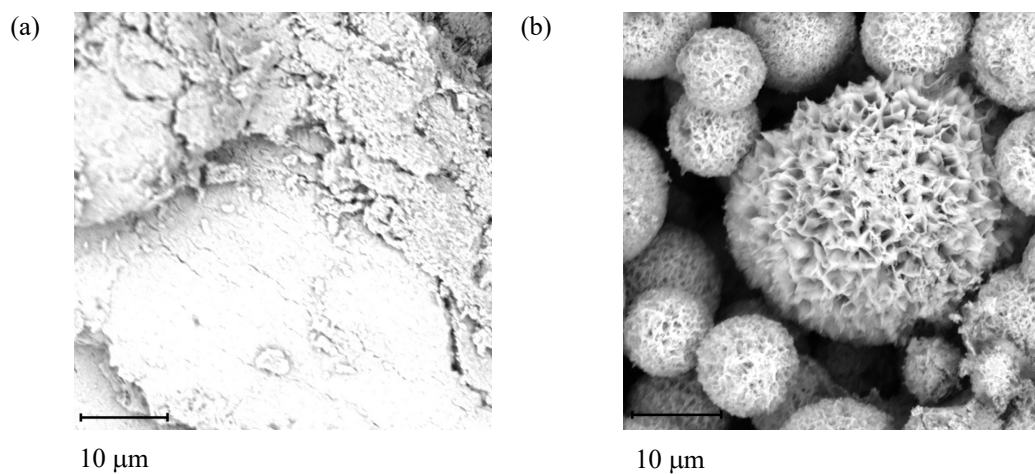


**Fig. 4** SEM images of crystals formed by mixing PBS and  $\text{CuSO}_4$  solution (a) without and (b) with *FBVMO*

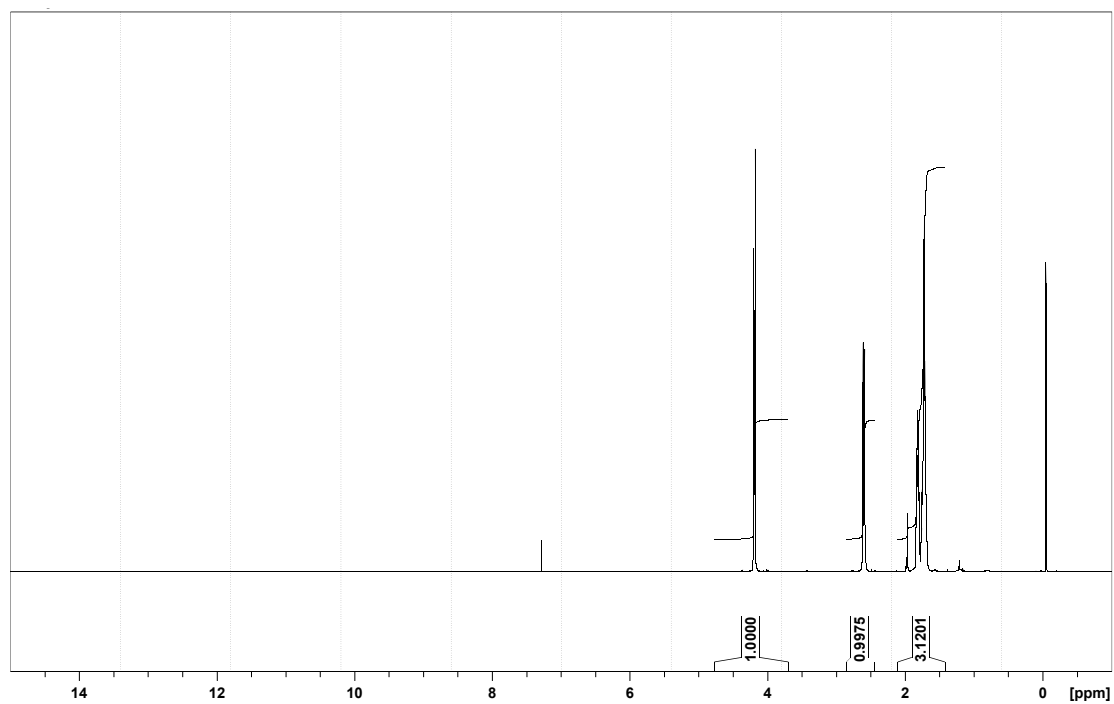


**Fig. 5**  $^1\text{H}$  NMR spectrum of  $\epsilon$ -caprolactone obtained by oxidation of cyclohexanone with immobilized *FBVMO*

## References

- Fraaije MW, Kamerbeek NM, van Berkel WJH, Janssen DB (2002) Identification of a Baeyer-Villiger monooxygenase sequence motif. *FEBS Lett* 518:43–47. [https://doi.org/10.1016/s0014-5793\(02\)02623-6](https://doi.org/10.1016/s0014-5793(02)02623-6)
- Rebehmed J, Alphanh V, de Berardinis V, de Brevern AG (2013) Evolution study of the Baeyer-Villiger monooxygenases enzyme family: functional importance of the highly conserved residues. *Biochimie* 95:1394–1402. <https://doi.org/10.1016/j.biochi.2013.03.005>
- Riebel A, Dudek HM, De Gonzalo G, et al (2012) Expanding the set of rhodococcal Baeyer-Villiger monooxygenases by high-throughput cloning, expression and substrate screening. *Appl Microbiol Biotechnol* 95:1479–1489. <https://doi.org/10.1007/s00253-011-3823-0>